FEBS Letters 581 (2007) 2675–2683

Intervention of geminiviral replication in yeast by ribozyme mediated downregulation of its Rep protein

Ushasri Chilakamarthi[a], Sunil K. Mukherjee[b,*], J.K. Deb[a,*]

[a] *Department of Biochemical Engineering and Biotechnology, Indian Institute of Technology, Delhi, Hauz Khas, New Delhi 110 016, India*
[b] *Plant Molecular Biology Division, International Centre for Genetic Engineering and Biotechnology, Aruna Asaf Ali Marg, New Delhi 110 067, India*

Received 23 November 2006; revised 20 April 2007; accepted 25 April 2007

Available online 15 May 2007

Edited by Shou-Wei Ding

Abstract **Geminiviruses pose serious threat to many economically important crops such as mungbean, tomato, cotton, etc. To devise a specific antiviral strategy at the viral DNA replication level, a hammerhead ribozyme was directed against the mRNA of the replication initiator protein (Rep). Rep is the most important viral protein for the DNA replication of the *Mungbean yellow mosaic India virus* (MYMIV), a member of the *Geminiviridae* family. The ribozyme showed ~33% cleavage activity on synthetic *rep* transcript within 1 h under in vitro conditions, whereas the mutant ribozyme, designed to lack the catalytic activity but target the same site, showed no cleavage. The in vivo efficiency of ribozyme was evaluated in *Saccharomyces cerevisiae* as it can act as a surrogate host for replication of the MYMIV-DNA and lacks RNAi machinery. In the presence of the ribozyme, growth of the yeast cells that are dependent on geminiviral replication was inhibited by 30% and cellular generation time was increased by 2 h. The RT-PCR analysis showed a maximum of about 50% reduction in the *rep* mRNA level in presence of the ribozyme compared to its noncatalytic mutant control. About 65% decrease in geminiviral DNA replication was observed due to the downregulation of replication initiator protein by the ribozyme. These results raise the possibility of engineering resistance to geminiviruses employing the ribozyme approach.**

Keywords: Geminivirus; Hammerhead ribozyme; Replication; Inhibition

1. Introduction

Geminiviruses are a large diverse family of ssDNA viruses that infect a broad variety of plants causing significant crop losses worldwide [1]. They replicate through double stranded DNA (dsDNA) intermediates in infected cells. Unlike RNA viruses, which code their own replicases, geminiviruses contribute only a few factors for their replication and transcription, and depend on DNA and RNA polymerases of their plant hosts. MYMIV is a member of genus *begomoviridae* with bipartite genome that is transmitted through whiteflies. The existing measures employed by farmers to eradicate geminiviruses are indirect, like controlling the population of alternate host or vectors such as whiteflies [2]. The whiteflies are unfortunately developing resistance to commonly used chemicals and the measures to control them are falling short. On the other hand, the geminiviral genomes are prone to recombination and thus the new, virulent virus strains evolve.

Searches have been going on for alternative antiviral strategies such as developing resistant cultivars either by classical crossbreeding or genetic engineering. Classical breeding techniques are laborious, time consuming and naturally resistant varieties are also limited in abundance. Earlier, there were attempts to endow plants with resistance against geminiviruses by using mutant or wild-type viral ORFs, antisense RNAs and RNA interference constructs, etc., as transgenes [3–6]. In most of the cases resistance was not up to the mark or limited to certain species [7,8]. The above strategies operate mostly through the RNA silencing pathways and plant's defense system might be compromised in the long run. In this scenario, we wanted to explore whether the ribozyme technology could be used as an alternative approach. As the different species of *geminiviridae* family share a common mode of rolling circle replication (RCR) [9–12], targeting viral replication machinery might be useful as a broad and durable control strategy in the fight against geminiviruses. In view of this the mRNA of replication initiator protein (Rep), the most important protein in viral DNA replication, has been chosen as the target for ribozyme activity. The replication initiator protein (Rep) makes a site specific nick in the plus strand of the replicative form at a conserved nonanucleotide site (TAATATT↓AC) that is present in the loop region of a hairpin spanning the replication origin sequences [13,14]. This nicking determines the initiation of RCR. The domain of nicking activity is located at the N-terminal of Rep protein. Three different mutations in a region of *rep* gene spanning nucleotides 128–152 inhibited DNA binding in vitro and DNA replication in vivo, thereby demonstrating the importance of this region and further supporting the close relationship between DNA binding and cleavage [15,16]. Therefore, targeting *rep* mRNA at this region might interfere with the expression of protein and in turn with viral replication. It may however be mentioned that though Rep initiates DNA replication in all geminiviruses, the *rep* gene sequences differ from one another. Hence finding a totally conserved region may be difficult.

Ribozymes are potential tools in the downregulation of gene expression. They act as molecular scissors by catalytically cleaving target RNAs, the molecular messages transmitted

*Corresponding authors. Fax: +91 11 26162316 (S.K. Mukherjee), +91 11 26582282 (J.K. Deb).
E-mail addresses: sunilm@icgeb.res.in (S.K. Mukherjee), jkdeb@dbeb.iitd.ac.in (J.K. Deb).

0014-5793/$32.00
doi:10.1016/j.febslet.2007.04.084

from the genes for production of proteins. Ribozyme can be divided into conserved catalytic domain responsible for catalysis and variable recognition domain responsible for the recognition of target [17,18]. The main advantage with ribozyme is that suitable changes in the recognition domain flanking the conserved catalytic core can essentially target any RNA. In the present study, we explored the *trans*-cleaving property of the hammerhead ribozyme targeted to the mRNA of replication initiator protein (Rep) of MYMIV, a member of the *Geminiviridae* family. This is the first report of the use of ribozyme strategy against geminiviruses.

2. Materials and methods

2.1. Microbial strains, plasmids, growth and selection media

The *E. coli* strain DH5α, used in this study to clone ribozyme mutant ribozyme, was obtained from Bethesda Research Laboratory, USA; and the *S. cerevisiae* (W303a) for in vivo expression of ribozymes was from EUROSCARF. The plasmids pSG1, pET28a, pGADC1, etc. were commercially available and the plasmid YCpO^{-}-2A was obtained from ICGEB, New Delhi. Luria Bertini broth (LB) contained bactopeptone, 1 g, NaCl, 1 g and Yeast Extract, 0.5 g per 100 ml of broth. The YPD medium contained Yeast Extract, 1 g, peptone, and glucose, 1 g each per 100 ml of broth. The 10× drop out medium (leu^{-}, his^{-}, trp^{-}, ade^{-}, ura^{-}) contained, L-tyr, L-isoleu, L- lys (300 mg each), L-arg, L-met (200 mg each), L-phe, 500 mg, L-val, 1.5 gm, L-thre, 2 gm per litre of broth. Ura, leu dropout medium contained Yeast nitrogen base 0.67 g, 10× drop out medium 10 ml, 40% glucose, 5 ml, 200× each of adenine, histidine and tryptophan 500 μl and 100× of uracil or leucine as desired. 200× adenine/tryptophan/histidine contained 400 mg per 100 ml solution. 100× leucine contained 1 g per 100 ml and 100× uracil contained 400 mg per 100 ml.

2.2. Design of ribozyme and mutant ribozyme

The prime requirement for cleavage by a hammerhead ribozyme is the presence of GUC triplet in the target RNA. Though hammerhead ribozyme recognizes and cleaves 3′ to NUX (where N is any ribonucleotide and X is A, U or C), the efficiency of NUX is low compared to GUC triplet [19]. Therefore, the target (Rep-mRNA) was scanned for the presence of GUC triplet to choose potential cleavage site and the search results yielded 16 GUC triplets in the entire length of *rep* transcript. Of all the GUC triplets listed, number 4 GUC triplet was chosen to demonstrate the proof of principle of ribozyme activity. Orozco and Hanley-Bowdoin created three different mutations in this region of TGMV *rep* and observed that all mutations inhibited DNA binding and cleavage in vitro and viral replication in vivo [16]. Targeting this region is likely to offer resistance against MYMIV and may establish the concept that ribozyme technology can be used as a potential tool in the battle against geminiviruses.

This region also contains GUC triplet, 3′ of which is putatively more cleavable by hammerhead ribozyme. Hence it has been chosen as a target site for ribozyme in our present study. The *trans*-cleaving hammerhead ribozyme consists of conserved catalytic core flanked by the base sequences, which are complementary to the target RNA sequences on either side of cleavage site (nucleotide C). In the present design, the complementary sequences spanned 13 and 12 nucleotides on the left and right of cleavage site respectively (Fig. 1b). These complementary sequences would direct ribozyme towards target and impart specificity to ribozyme. They bind the substrate molecule to form stem I and stem III of the hammerhead-substrate complex. A mutant ribozyme (disabled ribozyme) was constructed to the same target site as an antisense control in which double base pair mutations in the catalytic core of the ribozyme were introduced keeping rest of the sequence unaltered. The mutant ribozyme has similar antisense effect but lack catalytic cleavage activity. The sense and antisense oligonucleotides coding for ribozyme were chemically synthesized. The sequences are as follows.

The sense strand of ribozyme 5′ GAT CCA TCC GCA TCT GTT TCG TCC TCA CGG ACT CAT CGA GAG AAC TCC ATG 3′ (51-mer).

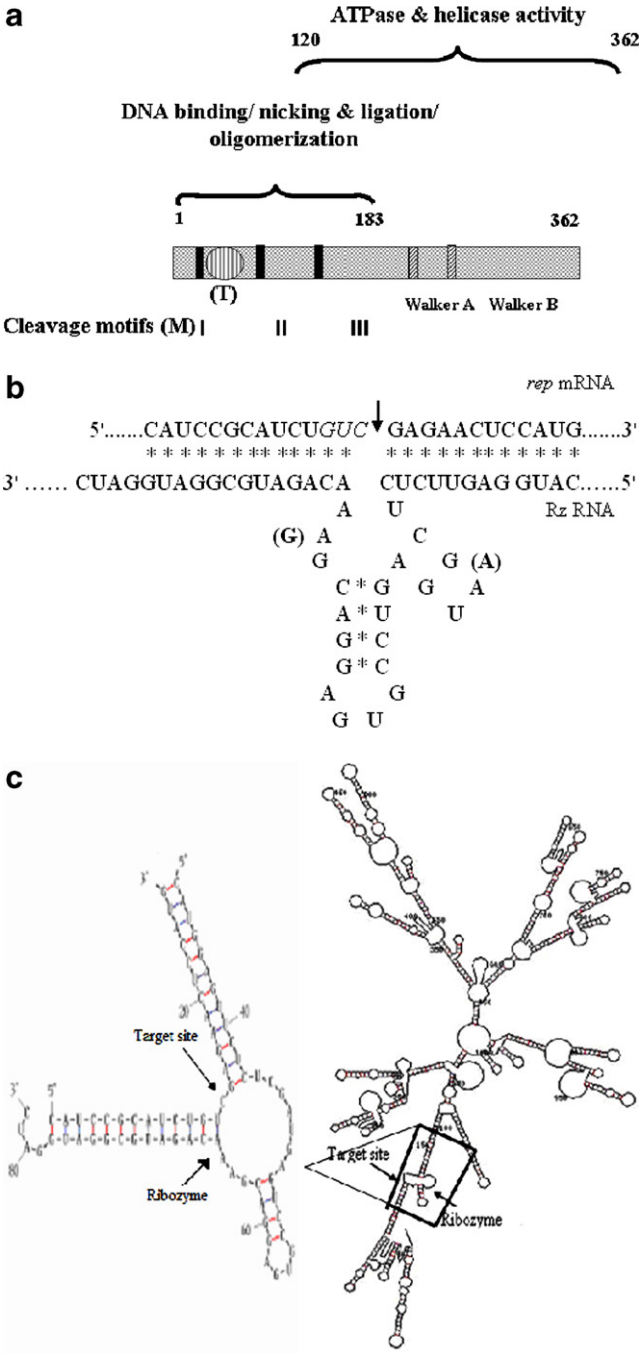

Fig. 1. Domain analysis of the *rep* gene and ribozyme. (a) The various structural and functional domains of *rep* are marked. The numbers indicate the position of the encoded amino acids. 'T' stands for the target site of the ribozyme. The symbols I, II, III indicate the conserved motifs for RCR. The design and validity of ribozyme molecule by secondary structure prediction are shown in (b) and (c). (b) Design of ribozyme and mutant ribozyme against Helix-2 region (T) of *rep*. The GUC triplet is shown in italics and arrow shows the cleavage site. The bases in parentheses are those present in the mutant ribozyme. (c) The secondary structure of full-length *rep* mRNA-ribozyme complex is shown in the right side of the panel. The black quadrilateral with an attached arrow represents the actual complex and is shown in the left side as a blow-up. The arrows show the target site of cleavage.

The antisense strand of ribozyme 5′ CAT GGA GTT CTC TCG ATG AGT CCG TGA GGA CGA AAC AGA TGC GGA TG 3′ (47-mer).

The sense strand of mutant ribozyme 5′ GAT CCA TCC GCA TCT GTT CCG TCC TCA CGG ACT CAT TGA GAG AAC TCC ATG 3′ (51-mer).

The antisense strand of mutant ribozyme 5′ CAT GGA GTT CTC TCA ATG AGT CCG TGA GGA CGG AAC AGA TGC GGA TG 3′ (47-mer).

One of the strands is engineered with BamHI overhang to facilitate directional cloning. The accessibility of hammerhead ribozyme to this region was examined using computer predicted secondary structure of *rep* mRNA-ribozyme complex by the software MFOLD version 2.3 [20] (http://www.bioinfo.rpi.edu/ ~ zukerm/seqanal/). It clearly showed that the ribozyme could not only access the target site but also formed its characteristic hammerhead structure upon binding to its substrate (Fig. 1c).

2.3. Construction of ribozyme, mutant ribozyme expression vectors

The chemically synthesized oligonucleotides were annealed and ligated to the double digested (SmaI and BamHI) pSGI vector downstream of T7 promoter (Fig. 2a) to facilitate in vitro transcription using T7 RNA polymerase (Promega, USA). The plasmids were designated as pSGIRz and pSGImRZ respectively for ribozyme and mutant ribozyme. For expressing ribozyme and mutant ribozyme in vivo in yeast, the respective annealed oligonucleotides were cloned under the control of Gal4 promoter in between SmaI and BglII sites of pGAD vector, and the resulting plasmids were designated as pGADRz and pGADmRz (Fig. 2b) respectively. For in vitro transcription, *rep* gene cloned in between the BamHI and HindIII sites of pET28a was used (Fig. 2c).

2.4. In vitro transcription and cleavage of rep transcript by ribozyme

The plasmids pSGIRz and pSGImRz were linearised with BamHI to carry out run off transcription. Linearisation with BamHI prevent transcription of the extra vector sequences that are 3′ to ribozyme-end. The plasmid pET28a-Rep was linearised with ClaI to produce 520 nt in vitro transcript (Fig. 2c). The in vitro transcription reaction was carried out using 1 μg of linearised DNA template, Riboprobe in vitro transcription kit (Promega), [α^{32}P] UTP (Specific activity 3000 Ci/mmol), following manufacturer's instructions. Following transcription, RQI RNase free DNase (1 U/μg of DNA template) was added and incubated at 37 °C for 15 min. The transcripts were purified by phenol:chloroform extraction and ethanol precipitation. The ribozyme, mutant ribozyme, and the target *rep* RNA were quantified spectrophotometrically by measuring absorbance at 260 nm. The *rep* RNA was quantified by trichloroacetic acid (TCA) precipitation of the radiolabeled transcript on glass fiber filters in presence of carrier tRNA followed by washing and counting in a liquid scintillation β counter (LKB, Wallac, 1219 Reckbeta). The target and ribozyme (or mutant) were mixed and cleavage reaction was carried out in a buffer containing 50 mM Tris–HCl, pH 7.5 in a volume of 10 μl. The reaction mixture was briefly heated at 94 °C and cleavage was initiated by adding $MgCl_2$ (10 mM, final concentration) at 37 °C for 1 h, referred to as standard cleavage conditions. The reaction was stopped at different time intervals by adding stop buffer (formamide, 95%, xylene cyanol and bromophenol blue, 0.05% each and EDTA, 20 mM). The samples were heated for 2 min at 75 °C and loaded on 6% denaturing PAGE to separate the target from the products. The gel was vacuum dried, exposed to X-ray film (BIOMAX™ MS, Kodak, USA) and the autoradiographic bands were quantified by Alpha Imager software (Bio-Rad). The percentage cleavage was calculated using formula $(P1 + P2)/(P1 + P2 + S) \times 100\%$, where S, P1 and P2 denote band intensities of substrate (520 nt *rep* transcript), product 1 (309 nt) and product 2 (211 nt), respectively.

2.5. Determination of kinetic parameters

Kinetic parameters of the ribozyme were determined by using varying concentrations of the labeled target *rep* RNA in the presence of constant amount of ribozyme as reported [21]. Hammerhead ribozymes obey simple Michaelis–Menton type kinetics [17]. Hence, kinetic parameters K_m and k_{cat} of ribozyme were determined following Michaelis–Menton kinetics. A fixed amount of unlabeled ribozyme (5 fmol) was allowed to react with varying concentrations of the labeled *rep* transcript under standard cleavage conditions at 37 °C. Hanes–Wolff's plot of substrate concentration over velocity versus substrate concentration [22] was used to determine values for Michaelis–Menten constant (K_m) and reaction rate at saturating substrate concentration (k_{cat}).

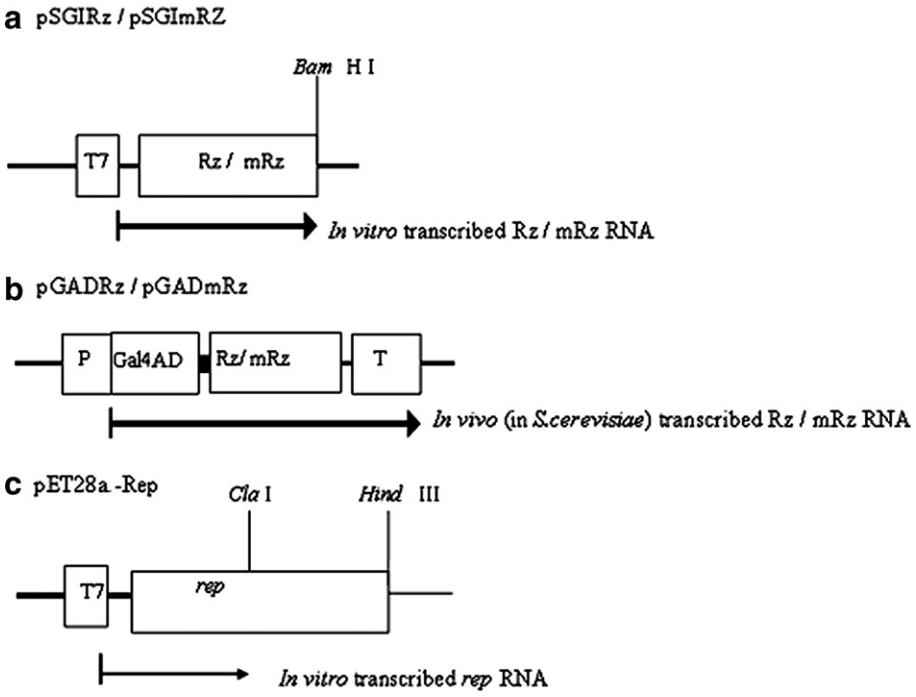

Fig. 2. Construction of ribozyme (Rz)/mutant ribozyme (mRz) and *rep* expression vectors. (a) Cloning of ribozyme/mutant ribozyme was carried out downstream of the T7 promoter. The black horizontal arrow represents the in vitro transcribed ribozyme or mutant ribozyme. (b) Cloning of Rz/mRz in pGAD under the control of Gal4 promoter and the in vivo transcribed Rz/mRz. T shows the transcription termination sequence. (c) Scheme of in vitro transcribed *rep* RNA from the Cla I digested fragment of pET28a-Rep plasmid.

2.6. Yeast transformation

The transformation of *S. cerevisiae* cells (W303a) with the plasmids was carried out using lithium acetate, single-stranded DNA, and polyethylene glycol [23]. The Ura auxotroph cells harbouring the plasmid YCpO$^-$-2A [27] (containing the Ura3 marker) was transformed with plasmids (pGAD or pGADRz or pGADmRz) containing Leucine marker, and the colonies were scored on synthetic defined (SD) Ura$^-$ Leu$^-$ plates. The extent of replication of plasmid YCpO$^-$-2A was controlled by the abundance of Rep protein in the yeast cells. The origin activity of plasmid YCpO$^-$-2A for each input plasmid was measured in terms of colony forming units (CFUs) in the Ura, Leu dropout plates when the equal moles of input DNA was applied in each transformation experiment.

2.7. Growth curve

Single colony of *S. cerevisiae* harbouring the desired plasmids was inoculated in 5 ml of respective drop out media and allowed to grow at 30 °C at 200 rpm. From the above primary cultures, cells were inoculated in 100 ml of respective drop out media and adjusted to the same O.D at 0 h. The growth was monitored at 3 h intervals for 24 h. Specific growth rate and doubling time were calculated from the growth curves using the formula $\log N/N_0 = \lambda t/2.303$, where N is number of cells at defined time point t, N_0 is the initial number of cells and λ is specific growth rate.

2.8. Reverse transcriptase- PCR (RT-PCR) analysis

First strand cDNA synthesis was carried out using 5 μg of total RNA prepared from *S. cerevisiae* harbouring various plasmids using ready to go T-primed first strand kit (Invitrogen). The tube containing the reaction mix (reaction buffer, dNTPs, Moloney Murine Leukemia Virus (M-MuLV) reverse transcriptase and an oligo (dT) primer) was kept at 42 °C for 10 min, RNA was denatured by heating at 65 °C for 5 min. The first strand reaction mix was reconstituted with the denatured RNA sample and placed at 42 °C for 60 min. The first cDNA thus prepared was directly used for PCR. *rep* gene specific primers (AL1 CS forward, AL1 Reverse) were used to amplify 530 bp fragment of *rep* gene. The amplified products were resolved by 1% agarose gel-electrophoresis. As an internal control, the *Rad54* housekeeping gene was also amplified using specific primers.

3. Results

In order to check the effectiveness of our strategy, it is desirable to test its ability to cleave the target initially under in vitro conditions before extending the study to in vivo conditions. Therefore, the following in vitro experiments were carried out to obtain data on the basic kinetic parameters of the ribozyme.

3.1. In vitro cleavage of rep transcript by ribozyme

The various domains of Rep protein including the ribozyme target site (T) have been shown in Fig. 1a. The putative linear and secondary structure of the Rep-ribozyme complex is shown in Fig. 1b and c respectively. The schematics of the constructs used for generating the *rep* and the ribozyme mRNAs in vitro are given in Fig. 2.

A time course of the cleavage reaction of *rep* RNA (10 fmol) with ribozyme (5 fmol) showed that ribozyme was able to cleave as early as 5 min of incubation (lane 3 in Fig. 3a). The cleavage efficiency increased with increasing incubation time till about 90 min. The percentage cleavage at different time points has been plotted in Fig. 3b. About 33% of the target RNA was cleaved after 60 min post incubation.

It is worth noting that the lanes 1–6 and lanes 7–10 of Fig. 3a have been spliced from the autoradiographs of two different gels. The splicing was necessary to get rid of the unnecessary portions of each of the gels that were electrophoresed and autoradiographed under same conditions. This splicing did not vitiate the interpretation or analysis of the data as the ribozyme activity was expressed not in absolute units but in terms of 'percentage of cleavage' only.

3.2. Determination of kinetic parameters

A fixed amount of unlabeled ribozyme (5 fmol) was allowed to react with varying concentrations of the labeled *rep* transcript under standard cleavage conditions at 37 °C (Fig. 3c). Since hammerhead ribozyme follows Michelis–Menten kinetcs, the kinetic parameters were calculated from Hanes–Wolff's plot (Fig. 3d). K_m and k_{cat} values for ribozyme were found to be 49.51 nM and 0.21 min^{-1}, respectively. On the basis of these data, the catalytic efficiency, i.e., the turn over number (k_{cat}/K_m) of 4.3×10^6 M^{-1} min^{-1} was obtained. The K_m and k_{cat} values so observed for the designed ribozyme are comparable to those of other ribozymes reported in literature [22,24–26] and relevant data are presented in Table 1.

3.3. Effect of pH and Mg^{2+} concentrations

It is known that the cleavage by hammerhead ribozyme is dependent upon divalent cations, the most common of which is Mg^{+2}, the cleavage activity was therefore studied at Mg^{+2} concentrations viz., 0–50 mM. The background cleavage was obtained in the absence of Mg^{2+} ions (lane 1 in Fig. 3e), which might result from Mg^{2+} carry over from in vitro transcription reaction. The efficiency of cleavage increased with increasing Mg^{+2} ion concentration from 0.5 mM to 50 mM. The cleavage efficiency of ribozyme also increased with increasing pH from 6 to 8.5 (Fig. 3f). This information was necessary to get an idea of the cleavage activity under normal physiological conditions of a eukaryotic cell.

3.4. In vivo efficiency of ribozyme in S. cerevisiae

The above in vitro results prompted us to examine the potential of ribozyme activity under physiological conditions. The *S. cerevisiae* was chosen as a model eukaryotic system to demonstrate in vivo ribozyme efficiency in inhibiting MYMIV DNA replication. Although, MYMIV is a plant pathogen, it has been shown that the MYMIV DNA- A is able to replicate in *S. cerevisiae* when cloned as a tandem dimer (YCpO$^-$-2A) in an ARS deficient plasmid YCpO$^-$ [27]. In other words, the DNA-A component conferred replication activity on this recombinant ARS deficient plasmid. The replication of the plasmid, recombinant with the viral DNA, was totally dependent on the viral *cis*-elements and the factors encoded by DNA-A. For example, the replication was severely down regulated if the viral origin of RCR was mutated, or if the initiator protein of RCR i.e., Rep was mutated (Y103F) [27].

3.4.1. Effect of ribozyme on the colony forming (CFU) ability of S. cerevisiae harbouring the YCpO$^-$-2A. The efficiency of ribozyme was evaluated in terms of the decreased ability of the yeast cells to form CFU following transformation with the ribozyme construct. In presence of the ribozyme, downregulation of the Rep expression and consequent dampening of the origin function of the plasmid YCpO$^-$-2A is expected. The loss in origin activity would be reflected in the diminution of CFU of the yeast cells expressing the ribozyme. The experiments were carried out with the *S. cerevisiae* cells harbouring YCpO$^-$-2A, which were transformed separately

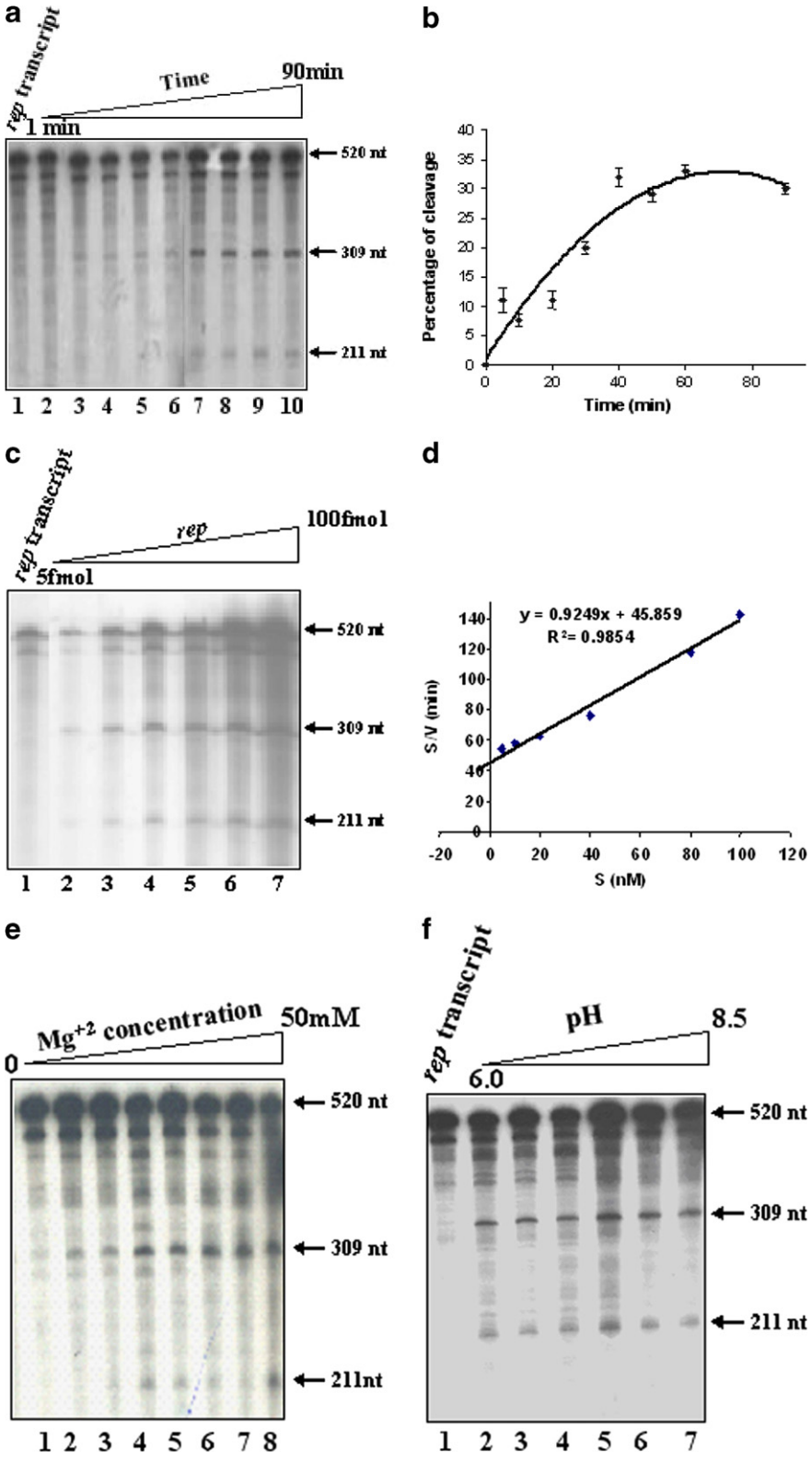

Fig. 3. In vitro cleavage reactions. (a) Autoradiogram showing kinetics of cleavage of *rep* RNA by ribozyme. Lane 1, *rep* transcript; the reaction time in lanes 2–10 is 1, 5, 10, 20, 30, 40, 50, 60 and 90 min, respectively. Arrows show the intact and the cleaved rep transcripts. (b) Percentage cleavage of *rep* by ribozyme at different time intervals. Percentage cleavage was calculated using the formula (P1 + P2)/(P1 + P2+S) × 100% where S, P1 and P2 denote band intensities of substrate (520 nt *rep* transcript), product 1 (309 nt) and product 2 (211 nt) as shown in (a). (c) Autoradiograph showing cleavage of varying concentrations of *rep* transcript with fixed concentration of ribozyme. Lane 1, 10 fmol of *rep* transcript (control), lanes 2–7 are 5, 10, 20, 40, 80, and 100 fmol, respectively of *rep* mRNA and 5 fmol of ribozyme. (d) Hanes–Wolff's plot of cleavage of *rep* transcript by ribozyme. (e) Autoradiogram showing cleavage of *rep* by ribozyme at varying $MgCl_2$ concentrations. Lanes 1–8, cleavage at 0, 0.5, 1, 2, 5, 10, 20 and 50 mM Mg^{+2} concentrations, respectively. (f). Autoradiogram showing cleavage of *rep* by ribozyme at varying pH of reaction buffer. Lane1, *rep* transcript at pH 7.5 (control); lanes 2–7, cleavage at 6.0, 6.5, 7, 7.5, 8 and 8.5 pH respectively.

Table 1
Comparison of kinetic parameters of *rep* ribozyme with other ribozymes reported in literature

Ribozyme targeted to	K_m (M)	k_{cat} (min^{-1})	k_{cat}/K_m ($\times 10^7$ M^{-1})	Reference
HEV	5.5×10^{-13}	1.2×10^{-5}	2.1	[24]
Di-Rz for HEV	2.5×10^{-13}	4.76×10^{-5}	19	
HPV-6b/11E1	14.7×10^{-9}	0.14	0.9	[25]
HBV	26.31×10^{-9}	0.18	0.6	[26]
Connective tissue growth factor mRNA	1.56×10^{-6}	2.97	0.19	[22]
Connective tissue growth factor mRNA	7.8×10^{-6}	5.7	0.073	[22]
rep of MYMIV	49.51×10^{-9}	0.216	0.043	Present study

with the plasmids pGAD or pGADRz or pGADmRz. The transforming plasmids were equalized in molar concentrations and the CFUs of the transformed cells were counted in the Ura and Leu dropout plates. The pGAD plasmid served as an empty vector control while the plasmid pGADmRz supplied the mutant ribozyme, defective in catalytic activity but retaining the similar antisense component (antisense control) as the functional ribozyme. The number of colonies counted with the pGAD vector was arbitrarily assigned a value of 100, and the other CFU numbers were scaled accordingly. The results are

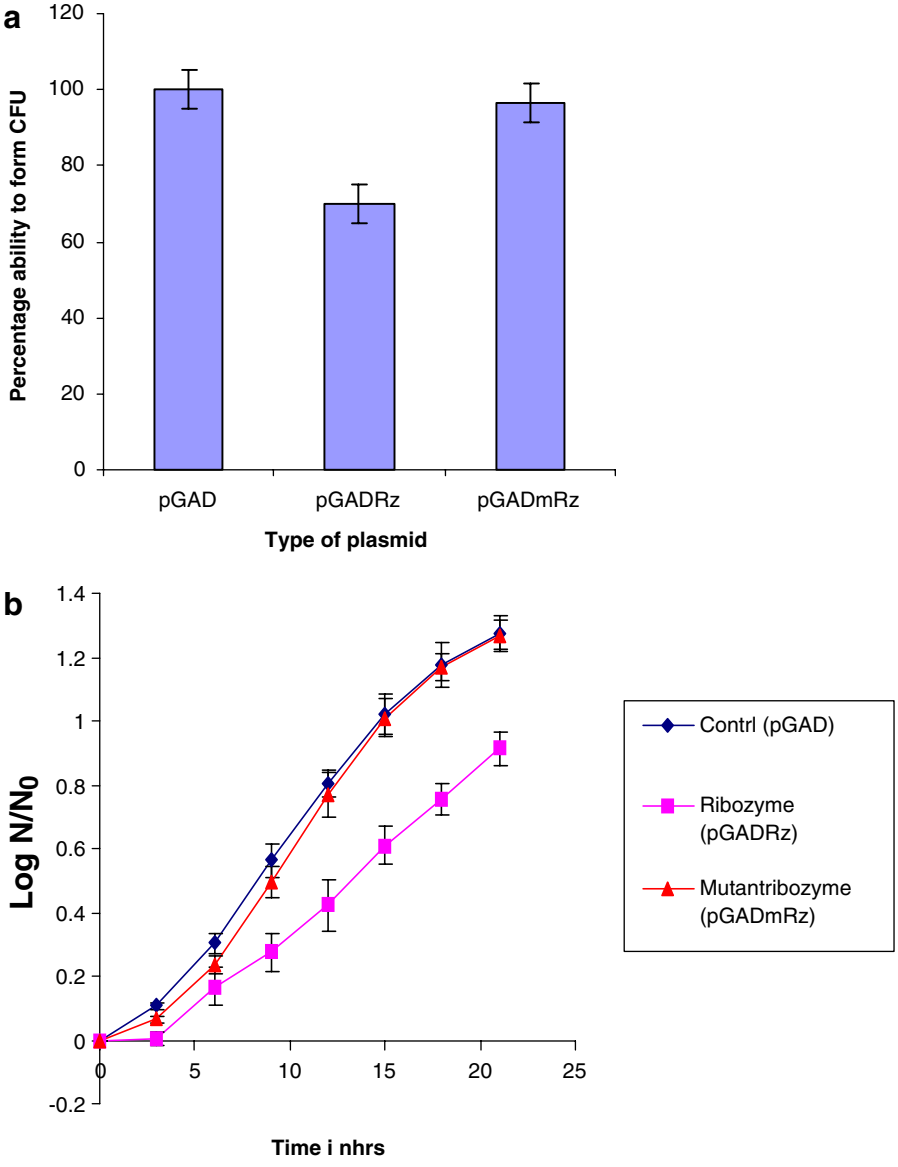

Fig. 4. Effect of ribozyme on growth of yeast. (a) Bar graph showing the percentage CFU. The CFUs represent the average numbers of tetra plicate experimental results. Black vertical lines show the error-bars. (b) Growth curve analysis of *S. cerevisiae* (harbouring YCpO$^-$-2A) transformed with pGAD or pGADRz or pGADmRz at 30 °C. *N* is number of cells at defined time period and N_0 is initial number of cells.

Table 2
Effect of ribozyme on the growth of *Saccharomyces cerevisiae* driven by geminiviral Rep

	Specific growth rate (h^{-1}) (λ)	Generation time (t)
pGAD	0.1549 ± 0.017	4 h 47 min
pGADmRz	0.1524 ± 0.02	4 h 54 min
pGADRZ	0.1061 ± 0.018	6 h 53 min

plotted in the form of a bar graph (Fig. 4a). These results indicated the reduction of 30% and 3.4% in CFU due to the activities of ribozyme and mutant ribozyme, respectively.

3.4.2. Effect of ribozyme on growth of S. cerevisiae. A growth curve analysis was carried out to observe the effect of ribozyme on the growth of *S. cerevisiae*. The growth was monitored at 3 h intervals for 24 h by measuring absorbance (A) at 600 nm and the growth curve is shown in Fig. 4b. The specific growth rate and generation time of *S. cerevisiae* cells harbouring the above mentioned plasmids (calculated from the growth curves as described in Section 2) are presented in Table 2. In presence of ribozyme, the generation time of yeast cells increased due to the drastic decrease in specific growth rate (Table 2). The presence of mutant ribozyme showed no significant difference in the values compared to control.

3.4.3. Reduction of rep mRNA in S. cerevisiae. To examine whether the reduction in CFU and the increase in generation time were due to ribozyme-mediated *rep* RNA cleavage, the levels of *rep* mRNA in the yeast cells were quantitated. The RT-PCR analysis was carried out to determine the *rep* mRNA level in *S. cerevisiae* cells harbouring the pGADRz or pGADmRz plasmids along with YCpO$^-$-2A. The *S. cerevisiae* cells were grown in the Leu$^-$Ura$^-$ broth overnight. Subsequently, the cultures were inoculated in YPD (complete medium) such that the initial $A_{600\,nm}$ in each case was identical. The cultures were pelleted at $A_{600\,nm}$ values 0.4, 0.6 and 1. Total RNA was isolated and the cDNA library was prepared. From the cDNA pool, 530 bp fragment of *rep* gene was amplified using *rep*-specific primers. The 1 kb fragment of *Rad54* gene was also amplified for internal loading control. The PCR-amplifications were carried out for 25 cycles (Fig. 5) and the intensity of the amplified bands was determined using Alpha Imager. A maximum of about 50% reduction in the expression of *rep* mRNA was observed in the case of cells transformed with pGADRz (lower band, Fig. 5c) compared to those transformed with pGADmRz (lower band, Fig. 5c). On the other hand, no difference in the *Rad54* mRNA (non-target mRNA) levels was observed in both types of cells. The suppression of *rep* RNA expression suggested that ribozyme was expressed well, could access and cleave its target. Diminution of *rep* mRNA levels in presence of ribozyme compared to its antisense control clearly indicated the strength of the wild-type catalytic activity.

3.4.4. Reduction in the accumulation of YCpO$^-$-2A plasmid. As mentioned earlier, replication of YCpO$^-$-2A was due to the Rep protein, coded by the same plasmid. In the presence of ribozyme, downregulation of *rep* RNA was observed (Fig. 5) and this, in turn, should adversely affect YCpO$^-$-2A replication. To test this, Southern hybridization was carried out to determine the level of YCpO$^-$-2A DNA. The *S. crevisiae* cells harbouring YCpO$^-$-2A and pGADRz or pGADmRz were grown overnight in Leu$^-$Ura$^-$ selection media. The cultures were inoculated in YPD (complete medium) and were adjusted to the same value of $A_{600\,nm}$. As the growth of each culture differs in the selection medium, we have taken complete medium to get the same number of cells and identical growth conditions for comparing replication of YCpO$^-$-2A plasmid DNA in the two cases. This would nullify the effect, if any, of the loss of plasmid due to lack of selection. The cultures were pelleted when $A_{600\,nm}$ reached ~1. Total DNA was isolated and subjected to hybridization using *rep* DNA as the probe to detect YCpO$^-$-2A DNA (upper bands in Fig. 5d). It was also probed with pGAD probe as an internal control to ascertain equal loading in both the wells (lower bands in Fig. 5d). The intensity of bands was quantified using phosphorimager. About 65% reduction of YCpO$^-$-2A DNA was observed due to ribozyme, pGADRz (upper band, Fig. 5d)

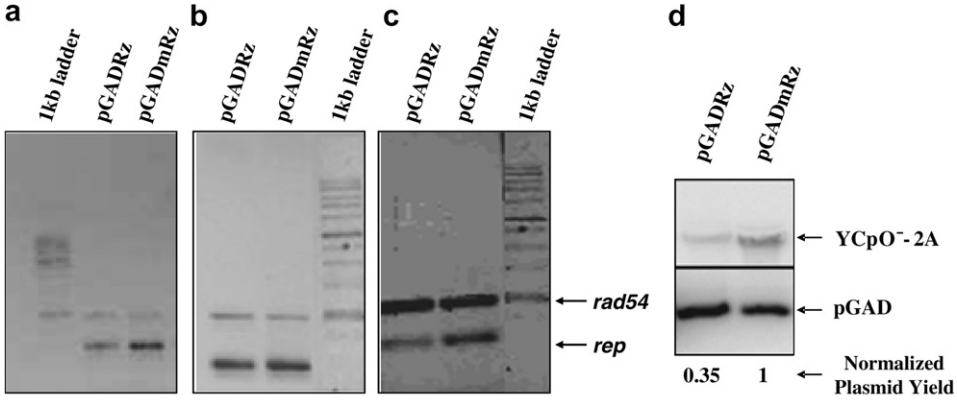

Fig. 5. Effect of ribozyme on *rep* mRNA levels and on accumulation of geminiviral DNA. (a–c) RT-PCR results showing *rep* mRNA expression levels when RNA was isolated at different growth stages (A_{600} = 0.4, 0.6 and 1, shown in panels a–c, respectively) of yeast harboring YCpO$^-$-2A along with pGADRz or pGADmRz. RT-PCR was carried out for 25 cycles in each case. In the presence of ribozyme, decrease in signal could be observed for 530 bp *rep* fragment at all growth stages. The RAD54 amplification (1 kb) is shown as internal loading control in all cases (upper bands). (d) Level of YCpO$^-$-2A plasmid DNA in *S. cerevisiae* harbouring ribozyme and mutant ribozyme. Total DNA of 10 μg was used for Southern hybridization. The *rep* DNA was used as probe to detect YCpO$^-$-2A (upper band). The same blot was reprobed with Gal4 fragment of pGAD (800 bp fragment of SphI and EcoRI digest of pGAD) to detect the levels of pGADRz and pGADmRz plasmids (lower bands, served as loading controls).

compared to its antisense control, pGADmRz (upper band, Fig. 5d). However, the levels of control plasmid (pGADRz or pGADmRz) remained same in both the cases (lower bands in Fig. 5d). These results clearly demonstrate the adverse effect of ribozyme on the replication of YCpO^{-}-2A.

4. Discussion

Hammerhead ribozymes have enormous potential as antiviral agents. We have designed anti *rep* ribozyme to target geminiviruses. The ribozyme designed to a region at 140 nt of *rep* showed about ~33% cleavage under in vitro conditions. Hammerhead ribozyme required divalent metal ions such as Mg^{+2} that participate in the mechanism of the cleavage reaction. Though considerable cleavage was obtained under in vitro conditions, it has been reported in literature that sometime ribozymes would fail to act in vivo because of low availability of Mg^{+2} ions in cellular environment. The fact that the ribozyme was effective at physiological Mg^{+2} (lane 4 in Fig. 3e) suggested its usefulness under in vivo conditions. Appreciable amount of cleavage was observed at all pH values including physiological pH (lane 5 in Fig. 3f) indicating its potential for in vivo applications. The kinetic parameters of ribozyme were calculated. The K_m values denote the affinity of ribozyme to its substrate while the k_{cat} values mostly reflect on the cleavage rate and multiple turnovers. Small flanking arm length of ribozyme generally facilitates multiple turnover events as its dissociation from the product can occur easily. However, it is difficult to compare the kinetic efficiencies of different ribozymes as the substrate molecules and their complexities change in each case.

Ribozymes directed to HEV had very high affinity and high turnover number among all the ribozymes presented in Table 1, in spite of low k_{cat} values. The most efficient wild type ribozymes display k_{cat}/K_m values of 10^8 M^{-1} min^{-1} [about the order of the apparent hybridization rate constant for two oligonucleotides [28]]. It has been suggested that within the intracellular environment, the hybridization step may be rate limiting for *trans*-acting ribozymes [27]. Kinetic and mutagenesis experiments have indicated that for both natural and engineered ribozymes, product release may be rate limiting at substrate saturation condition [29,30]. This limitation could be due to the increased length of the complementary sequence of RNA to which the ribozyme hybridizes.

The ribozyme reported here exhibited K_m in nM range, which was quite satisfactory, though not very low like the HEV ribozyme. The k_{cat} values were also comparable with the ribozymes targeted to HPV-6b/11E1 and HBV, but less than those directed to connective tissue growth factor RNA (Table 1). The decrease in hybridizing arm length might increase the k_{cat} value. In our design, the right hand flanking arms consists of 12 nucleotides forming helix I and the left arm spans 13 nucleotides of the helix III in hammerhead-substrate complex. These 25 bases of complementary sequence allow more efficient loading of ribozyme at the target site, but impede dissociation of ribozyme from the products, thus decreasing the number of turnover events. However, in our design, long complementary sequences are necessary as part of target site is involved in base pairing in the secondary structure of *rep* mRNA as predicted by the MFOLD program. These long complementary sequences unfold the secondary structure of target and help ribozyme to bind to the target site, which is otherwise inaccessible. The in vitro results confirmed the accessibility of target site to ribozyme and sequence specificity of cleavage.

Earlier, attempts were made to use ribozyme technology against plant viruses. Liu et al. [31] used hammerhead ribozyme against plant virus Plum poxvirus. It was expressed episomally in *N. clevelandii* by infection with recombinant Potatovirus X (PVX). They used 400 nt antisense RNA as antisense control. The protective effect was stronger in the case of ribozyme than the ordinary antisense RNA at one week after inoculation. However, eventually all plants tested accumulated comparable titers of PPV. The authors speculated that spatial separation of target and ribozyme might be the possible reason for the failure of ribozyme in this case. It was shown by De Feyter et al. [32] that the chromosomal expression of a catalytic antisense RNA directed against TMV resulted in protection, but that the catalytic domain of the hammerhead ribozyme was actually not required for this effect, resembling the phenomenon of RNA mediated protection and co-suppression. Keeping such facts in mind, the ribozyme efficiency was studied first in *S. cerevisiae*, wherein the RNA interference machinery is absent. Moreover, the *S. cerevisiae* system offers easy and rapid eukaryotic assay platform to monitor the efficiency of ribozyme compared to plants as raising transgenic plant and observing the phenotypes at the F1 and F2 generations is laborious as well as time consuming. Based on the positive results, the study could be further extended to more difficult system, such as plants. The data revealed that the ribozyme-mediated downregulation of *rep* RNA affected replication of the plasmid bearing the MYMIV DNA replication origin sequences. Consequently, the growth of *S. cerevisiae* in selection medium was affected as revealed by the decrease in formation of CFU and increase in generation time. This downregulation is a clear indicator of the ribozyme activity in vivo. The amount of in vitro cleavage (~33%) matched well with the amount of reduction (~50%) of *rep* mRNA within yeast. Plant level experiments with transient expression of ribozyme has been carried out. The wild type ribozyme inactivated the *rep* transcript (data not shown). Such observations call for exploring the ribozymes that are more potent than the ones reported here and also raise the hope that the ribozymes, when present in plants, might act as a tool for geminivirus resistance.

In conclusion, it may be mentioned that though Rep protein initiates DNA replication in all geminiviruses, the *rep* gene sequences differ from one another. As already mentioned, finding totally conserved region is also difficult. Nevertheless, the present study demonstrates for the first time the effectiveness of using hammerhead ribozyme in the inactivation of a vital function of geminivirus. A better target may be the coat protein 'CP' of begomoviruses from the point of view of the conservation of target sites.

Acknowledgements: The authors express their thanks to Dr. A.C. Banerjee, National Institute of Immunology, New Delhi, for his advice and active support in the execution of some experiments. One of us (Ch.U) is grateful to C.S.I.R., Government of India, New Delhi for financial support in the form of Senior Research Fellowship.

References

[1] Hanley-Bowdoin, L., Settlage, S.B., Orozco, B.M., Nagar, S. and Robertson, D. (1999) Geminiviruses: models for plant DNA

replication, transcription, and cell cycle regulation. Crit. Rev. Plant Sci. 35, 105–140.
[2] Varma, A., Dhar, A.K. and Mandal, B. (1992) MYMV transmission and control in India. In: Mungbean Yellow Mosaic Disease: Proceedings of an International Workshop, Asian Vegetable Research and Development Centre, Taipei, pp. 8–27.
[3] Asad, S., Haris, W.A., Bashir, A., Zafar, Y., Malik, K.A., Malik, N.N. and Lichtenstein, C.P. (2003) Transgenic tobacco expressing geminiviral RNAs are resistant to the serious viral pathogen causing cotton leaf curl disease. Arch. Virol. 148, 2341–2352.
[4] Chellappan, P., Masona, M.V., Vanitharani, R., Taylor, N.J. and Fauquet, C.M. (2004) Broad spectrum resistance to ssDNA viruses associated with transgene-induced gene silencing in cassava. Plant Mol. Biol. 56, 601–611.
[5] Hou, Y.M., Sanders, R., Ursin, V.M. and Gilberston, R.L. (2000) Transgenic plants expressing geminivirus movement proteins: abnormal phenotypes and delayed infection by Tomato mottle virus in transgenic tomatoes expressing the Bean dwarf mosaic virus BV1 or BC1 proteins. Mol. Plant-Microbe Interact. 13, 297–308.
[6] Zhang, P., Vanderschuren, H., Fütterer, J. and Gruissem, W. (2005) Resistance to cassava mosaic disease in transgenic cassava expressing antisense RNAs targeting virus replication genes. Plant Biotechnol. 3, 385–397.
[7] Brunetti, A., Tavazza, R., Noris, E., Lucioli, A., Accotto, G.P. and Tavazza, M. (2001) Transgenically expressed T-Rep of tomato yellow leaf curl Sardinia virus acts as a *trans*-dominant-negative mutant, inhibiting viral transcription and replication. J. Virol. 75, 10573–10581.
[8] Lucioli, A., Noris, E., Brunetti, A., Tavazza, R., Ruzza, V., Castillo, A.G., Bejarano, E.R., Accotto, G.P. and Tavazza, M. (2003) *Tomato yellow leaf curl Sardinia virus* Rep-derived resistance to homologous and heterologous geminiviruses occurs by different mechanisms and is overcome if virus-mediated transgene silencing is activated. J. Virol. 77, 6785–6798.
[9] Saunders, K., Lucy, A. and Stanley, J. (1991) DNA forms of the geminivirus African cassava mosaic virus consistent with a rolling circle mechanism of replication. Nucleic Acids Res. 19, 2325–2330.
[10] Stenger, D.C., Revington, G.N., Stevenson, M.C. and Bisaro, D.M. (1991) Replicational release of geminivirus genomes from tandemly repeated copies: evidence for rolling-circle replication of a plant viral DNA. Proc. Natl. Acad. Sci. USA 88, 8029–8033.
[11] Heyraud, F., Matzeit, V., Kammann, M., Schaefer, S., Schell, J. and Gronenborn, B. (1993) Identification of the initiation sequence for viral strand DNA synthesis of wheat dwarf virus. EMBO J. 12, 4445–4452.
[12] Heyraud, F., Matzeit, V., Kammann, M., Schaefer, S., Schell, J. and Gronenborn, B. (1993) The conserved nonanucleotide motif of the geminivirus stem loop sequence promotes replicational release of virus molecules from redundant copies. Biochimie 75, 605–615.
[13] Stanley, J. (1995) Analysis of African cassava mosaic virus recombinants suggests strand nicking occurs within the conserved nonanucleotide motif during the initiation of rolling circle DNA replication. Virology 206, 707–712.
[14] Laufs, J., Jupin, I., David, C., Schumacher, S., Heyraud-Nitschke, F. and Gronenborn, B. (1995) Geminivirus replication: genetic and biochemical characterization of Rep protein function, a review. Biochimie 77, 765–773.
[15] Orozco, B.M., Miller, A.B., Settlage, S.B. and Hanley-Bowdoin, L. (1997) Functional domains of a geminivirus replication protein. J. Biol. Chem. 272, 9840–9846.
[16] Orozco, B.M. and Hanley-Bowdoin, L. (1998) Conserved sequence and structural motifs contribute to the DNA binding and cleavage activities of a geminivirus replication protein. J. Biol. Chem. 273, 24448–24456.
[17] Uhlenbeck, O. (1987) A small catalytic oligoribinucleotide. Nature 328, 596–600.
[18] Haseloff, J. and Gerlach, W.L. (1988) Simple RNA enzymes with new and highly specific endoribonuclease activities. Nature 334, 585–591.
[19] Shimayana, T., Nishikawa, S. and Taira, K. (1995) Generality of the NUX rule: Kinetic analysis of the results of systematic mutations in the trinucleotide at the cleavage site of hammerhead ribozyme. Biochemistry 34, 3649–3654.
[20] Zuker, M. (1989) On finding all suboptimal foldings of an RNA molecule. Science 244, 48–52.
[21] Santoro, S.W. and Joyce, G.F. (1997) A general purpose RNA-cleaving DNA enzyme. Proc. Natl. Acad. Sci. USA 94, 4262–4266.
[22] Blalock, T.D., Yuan, R., Lewin, A.S. and Schultz, G.S. (2004) Hammerhead ribozyme targeting connective tissue growth factor mRNA blocks transforming growth factor-beta mediated cell proliferation. Exp. Eye Res. 78, 1127–1136.
[23] Agatep, R., Kirkpatrick, R.D., Parchaliuk, D.L., Woods, R.A. and Gietz, R.D. (1998) Transformation of *Saccharomyces cerevisiae* by lithium acetate/ single stranded DNA/polyethylene glycol (LiAc/ss-DNA/PEG) protocol. Technical Tips Online [Online.] http://tto.trends.com.
[24] Sriram, B., Thakral, D. and Panda, S.K. (2003) Targeted cleavage of hepatitis E virus 3'end RNA mediated by hammerhead ribozyme inhibits viral RNA replication. Virology 312, 350–358.
[25] Liu, D.Z., Jin, Y.X., Hou, H., Huang, Y.Z., Yang, G.C. and Qian, C. (1999) Preparation and identification of activity of anti HPV-6b/11E1 universal ribozyme Rz1198 *in vitro*. Asian J. Androl. 1, 195–201.
[26] Hu Song, Y., Sheng Lin, J., Zhi Liu, N., Juan Kong, X., Xie, N., Xia Wang, N. and Xin Jin, Y. (2002) Anti-HBV hairpin ribozyme-mediated cleavage of target RNA *in vitro*. World J. Gastroenterol. 8, 91–94.
[27] Raghavan, V., Malik, P.S., Choudhury, N.R. and Mukherjee, S.K. (2004) The DNA-A component of plant geminivirus (Indian Mung Bean Yellow Mosaic Virus) replicates in budding yeast cells. J. Virol. 78, 2405–2413.
[28] Cech, T.R. (1992) Ribozyme engineering. Curr. Opin. Struct. Biol. 2, 605–609.
[29] Bedrtrand, E., Pictet, R. and Grange, T. (1993) Can the hammerhead ribozymes be efficient tools to inactivate gene function? Nucleic Acids Res. 22, 293–300.
[30] Herschlag, D. (1991) Implications of ribozyme kinetics for targeting the cleavage of specific RNA molecules *in vivo*: more isn't always better. Proc. Natl. Acad. Sci USA 88, 6921–6925.
[31] Liu, B., Tabler, M. and Tsagris, M. (2000) Episomal expression of a hammerhead ribozyme directed against plum pox virus. Virus Res. 68, 15–23.
[32] De Feyter, R., Young, M., Schroeder, K., Dennis, E.S. and Gerlach, W. (1996) A ribozyme gene and an antisense gene are equally effective in conferring resistance to tobacco mosaic virus on transgenic tobacco. Mol. Gen. Genet. 250, 329–338.